Available online at www.sciencedirect.com
SCIENCE DIRECT®
Journal of Chromatography A, 1028 (2004) 75–88
JOURNAL OF CHROMATOGRAPHY A
www.elsevier.com/locate/chroma

# Physical origin of peak tailing on $C_{18}$-bonded silica in reversed-phase liquid chromatography

Fabrice Gritti [a,b], Georges Guiochon [a,b,*]

[a] *Department of Chemistry, University of Tennessee, Knoxville, TN 37996-1600, USA*
[b] *Division of Chemical Sciences, Oak Ridge National Laboratory, Oak Ridge, TN 37831-6120, USA*

Received 26 September 2003; received in revised form 27 October 2003; accepted 19 November 2003

**Abstract**

Single component isotherm data of caffeine and phenol were acquired on two different stationary phases for RPLC, using a methanol/water solution (25%, v/v, methanol) as the mobile phase. The columns were the non-endcapped Waters Resolve-$C_{18}$, and the Waters XTerra MS $C_{18}$. Both columns exhibit similar $C_{18}$-chain densities (2.45 and 2.50 μmol/m$^2$) and differ essentially by the nature of the underivatized solid support (a conventional, highly polar silica made from water glass, hence containing metal impurities, versus a silica–methylsilane hybrid surface with a lower density of less acidic free silanols). Thirty-two adsorption data points were acquired by FA, for caffeine, between $10^{-3}$ and 24 g/l, a dynamic range of 24,000. Twenty-eigth adsorption data points were acquired for phenol, from 0.025 to 75 g/l, a dynamic range of 3000. The expectation-maximization procedure was used to derive the affinity energy distribution (AED) from the raw FA data points, assuming a local Langmuir isotherm. For caffeine, the AEDs converge to a bimodal and a quadrimodal distribution on XTerra MS-$C_{18}$ and Resolve-$C_{18}$, respectively. The values of the saturation capacity ($q_{s,1} \simeq 0.80$ mol/l and $q_{s,2} \simeq 0.10$ mol/l) and the adsorption constant ($b_1 \simeq 3.1$ l/mol and $b_2 \simeq 29.1$ l/mol) measured on the two columns for the lowest two energy modes 1 and 2, are comparable. These data are consistent with those previously measured on an endcapped Kromasil-$C_{18}$ in a 30/70 (v/v), methanol/water solution ($q_{s,1} = 0.9$ mol/l and $q_{s,2} = 0.10$ mol/l, $b_1 = 2.4$ l/mol and $b_2 = 16.1$ l/mol). The presence of two higher energy modes on the Waters Resolve-$C_{18}$ column ($q_{s,3} \simeq 0.013$ mol/l and $q_{s,4} \simeq 2.6\ 10^{-4}$ mol/l, $b_3 \simeq 252$ l/mol and $b_4 = 13{,}200$ l/mol) and the strong peak tailing of caffeine are explained by the existence of adsorption sites buried inside the $C_{18}$-bonded layer. It is demonstrated that strong interactions between caffeine and the water protected bare silica surface cannot explain these high-energy sites because the retention of caffeine on an underivatized Resolve silica column is almost zero. Possible hydrogen-bond interactions between caffeine and the non-protected isolated silanol groups remaining after synthesis amidst the $C_{18}$-chain network cannot explain these high energy interactions because, then, the smaller phenol molecule should exhibit similarly strong interactions with these isolated silanols on the same Resolve-$C_{18}$ column and, yet, the consequences of such interactions are not observed. These sites are more consistent with the heterogeneity of the local structure of the $C_{18}$-bonded layer. Regarding the adsorption of phenol, no matter whether the column is endcapped or not, its molecular interactions with the bare silica were negligible. For both columns, the best adsorption isotherm was the Bilangmuir model (with $q_{s,1} \simeq 2$ and $q_{s,2} \simeq 0.67$ mol/l, $b_1 \simeq 0.61$ and $b_2 \simeq 10.3$ l/mol). These parameters are consistent with those measured previously on an endcapped Kromasil-$C_{18}$ column under the same conditions ($q_{s,1} = 1.5$ and $q_{s,2} = 0.71$ mol/l, $b_1 = 1.4$ l/mol and $b_2 = 11.3$ l/mol). As for caffeine, the high-energy sites are definitely located within the $C_{18}$-bonded layer, not on the bare surface of the adsorbent.


*Keywords:* Adsorption equilibrium; Frontal analysis; Peak tailing; Affinity energy distribution; Silanol activity; Column heterogeneity; Overloaded band profiles; Caffeine; Phenol; Silica

## 1. Introduction

The position and shape of overloaded band profiles recorded in preparative liquid chromatography depends directly on the adsorption equilibrium isotherm of the compound between the stationary and the mobile phases. This observation is valid provided that the column efficiency is high enough. The experimental determination of the adsorption isotherm represents the key task if anyone wants to predict accurately overloaded band profiles and perform computer assisted optimization and/or method development in preparative chromatography [1–3]. This

* Corresponding author. Tel.: +1-865-974-0733; fax: +1-865-974-2667.
*E-mail address:* guiochon@utk.edu (G. Guiochon).

0021-9673/$ – see front matter © 2004 Elsevier B.V. All rights reserved.
doi:10.1016/j.chroma.2003.11.090

ultimately permits an important cost reduction by saving time and chemicals with respect to what any empirical approach requires and by approaching closer the optimum conditions [1]. A fundamental understanding of the adsorption process involved in a separation is not a necessary constraint for the acquisition of meaningful equilibrium isotherm data nor for their accurate modeling. A close agreement between the experimental and the calculated band profiles is all that is required for the determination of good estimates of the experimental conditions under which the objective function is optimum. It is not yet fully realized how, provided that it is applied with due caution, the measurement, the modeling, and the interpretation of equilibrium adsorption data can help in reaching a far deeper understanding of the adsorption mechanisms involved in a particular separation. The difficulties encountered consist in recognizing what, in the results obtained, is specific of the separation studied and what is more general, and in distinguishing between the fundamental properties hinted at by the models used and the empirical relationships that they suggest. One of these difficulties that is often encountered requires to ascertain what features of the equilibrium isotherm model make physical sense, are consistent with the actual properties of the surface of the adsorbent studied, its heterogeneity, or whether the values of the thermodynamic constants of adsorption measured are consistent with the known values of the interaction energies.

We have shown previously that the selection of an isotherm model based only on the statistical results of the fitting procedure of the adsorption data acquired by a most accurate method like frontal analysis (FA) does not always give the most physically meaningful model [4,5]. Giving a small fitting residual in the regression of the data is a necessary conditions not a sufficient one for the selection of the most satisfactory equilibrium isotherm model. Besides the regression to an isotherm equation, other, independent treatments of the adsorption data can be useful and should be performed. For instance, the affinity energy distribution (AED) or distribution of the energy of interaction between the solute and the adsorbent (the surface of which is always somewhat heterogeneous) can be derived from the raw adsorption data, as shown by Stanley et al. who developed the numerical expectation-maximization procedure [6]. This method has the advantage of introducing no spurious information. It was successfully used to determine the general isotherm behavior of phenol on a Kromasil-$C_{18}$ column for methanol/water mobile phase compositions ranged between 0 and 60% [7–9]. Using this model, overloaded band profiles were predicted with close agreement with experimental data, in a wide range of gradient conditions, demonstrating the accuracy of the isotherm model [9]. The conclusions of this work regarding the adsorption of phenol were that there are two distinct types of adsorption sites on the surface of Kromasil-$C_{18}$ with different adsorption energies. The higher the water content in the mobile phase, the larger the number of the high-energy sites on the surface [7]. This is consistent with the evolution of the $C_{18}$-layer structure at high water content, leading ultimately to the collapse of these chains in pure water.

The physical interpretation of these two distinct sites on the Kromasil-$C_{18}$ surface was not elucidated in this early work [4–9] but we have suggested a mechanism explaining the existence of the bimodal energy distribution of phenol on this column [10]. We measured the adsorption isotherm of phenol and caffeine on six different commercial brands of endcapped $C_{18}$-bonded silica, to understand better the general retention mechanism of these two compounds in RPLC. Whatever the solute and the column considered, the AED converges toward a bimodal distribution. Accordingly, the best isotherm model is the Bilangmuir model. Two important conclusions were drawn from our results: (1) the low energy sites are located at the very interface between the stationary and the mobile phases, i.e., they are on the top of the $C_{18}$ layer; (2) the high-energy sites are deeply buried in the $C_{18}$-bonded layer, they are not residual silanols or dissociated silanophilic groups found on the exposed bare silica surface. This last conclusion was essentially based on the small difference between the energies of the two types of adsorption sites, 5 kJ/mol. This conclusion was logical but not definitive because no data were measured for the adsorption of phenol and caffeine on bare silica. The high-energy sites could be explained by interactions between the solutes and some residual silanols.

In this work, we investigate whether or not the high-energy adsorption sites encountered by phenol and caffeine can be explained by some interactions with the bare surface of the adsorbent. For this purpose, we measured, modeled, and compared the adsorption isotherms of phenol and caffeine on two specifically chosen stationary phases, one with practically no silanol groups, XTerra-$C_{18}$, the other one with a high density of such groups, Resolve-$C_{18}$. The first material is the new $C_{18}$ derivatized silica-methylsilane hybrid surface elaborated by Waters (Milford, MA, USA), which has no residual silanols at pH lower than 10 [11]. The second material is the $C_{18}$ derivatized Resolve silica that still contains approximately 70% of the silanols of the underivatized Resolve silica. The bonding of the $C_{18}$ chains to the Resolve Silica does not alter the acidity of the surface silanols [11]. Finally, analytical injections were performed on a column of underivatized Resolve Silica. The adsorption energies of the two compounds estimated from their retention factors on this underivatized silica were compared with those measured on the Resolve-$C_{18}$ column. The two $C_{18}$-bonded columns studied can be considered as being at the two extremes of the range of silanophilic activity of RPLC stationary phases and seemed to be the most appropriate columns to investigate the possible effects of the bare silica surface exposed to the adsorption of phenol and caffeine in RPLC and the nature of the high-energy sites found in RPLC columns.

## 2. Theory

### 2.1. Determination of the adsorption isotherms by frontal analysis (FA)

Frontal analysis (FA) was used to measure the single-component adsorption isotherm data of phenol and caffeine [1,12,13]. It consists in the abrupt replacement of the stream of mobile phase percolating through the column with a stream of a solution of the studied compound in the same mobile phase. The breakthrough curve is recorded, the column is washed with the pure mobile phase, and the experiment is repeated with a more concentrated solution. Mass conservation of the solute between the times when the new solution enters the column and when the plateau concentration is reached allows the calculation of the mass, $m_t^*$, of solute retained in the column at equilibrium with a given mobile phase concentration, $C$. This mass is best measured by integrating the breakthrough curve (equal area method) [14]. The amount $m_t^*$ is given by:

$$m_t^* = CV_{eq} \tag{1}$$

where $V_{eq}$ is the elution volume of the equivalent area of the solute. Note that $m_t^*$ is not the mass of solute adsorbed but the total mass present in the whole column at the end of the experiment, either adsorbed or in solution in the void volume. The knowledge of this latter volume (i.e. the volume inside the column that is available to the solution of concentration $C$) allows the determination of the adsorbed amount $q_a^*$ per unit of adsorbent volume by:

$$q_a^* = \frac{m_t^* - CV_0}{V_a} \tag{2}$$

where $V_0$ and $V_a$ are the column void volume and the adsorbent volume, respectively. The adsorption data consist in the set of pairs $q_a^*$, $C$ acquired.

### 2.2. Models of isotherm

Three isotherm models were used to describe the adsorption isotherm of phenol and caffeine. All three models are based on the Langmuir model. They are the Bilangmuir, and two further extensions, the Trilangmuir and the Quadrilangmuir isotherm models. The Bilangmuir model is the simplest model for a nonhomogeneous surface [15]. It can easily be extended to a Trilangmuir or a Quadrilangmuir model. The surface is assumed to be paved with two, three or four different types of homogeneous chemical domains which behave independently. Then, the equilibrium isotherm results from the addition of two, three or four independent local Langmuir isotherms:

$$q^* = q_{s,1}\frac{b_1 C}{1+b_1 C} + q_{s,2}\frac{b_2 C}{1+b_2 C} \tag{3}$$

for the Bilangmuir isotherm,

$$q^* = q_{s,1}\frac{b_1 C}{1+b_1 C} + q_{s,2}\frac{b_2 C}{1+b_2 C} + q_{s,3}\frac{b_3 C}{1+b_3 C} \tag{4}$$

for the Trilangmuir isotherm and

$$q^* = q_{s,1}\frac{b_1 C}{1+b_1 C} + q_{s,2}\frac{b_2 C}{1+b_2 C} + q_{s,3}\frac{b_3 C}{1+b_3 C} + q_{s,4}\frac{b_4 C}{1+b_4 C} \tag{5}$$

for the Quadrilangmuir isotherm.

In these models, there are one, two, three or four saturation capacities, $q_{s,1}$, $q_{s,2}$, $q_{s,3}$ and $q_{s,4}$, that are related to the surface area of each one of the different types of sites existing on the surface. The equilibrium constants $b_1$, $b_2$, $b_3$, and $b_4$ are associated with the adsorption energies $\epsilon_{a,1}$, $\epsilon_{a,2}$, $\epsilon_{a,3}$, and $\epsilon_{a,4}$, through the following equation [16]:

$$b_i = b_0 e^{\epsilon_{a,i}/RT} \tag{6}$$

where $\epsilon_{a,i}$ is the energy of adsorption, $R$ is the universal ideal gas constant, $T$ is the absolute temperature and $b_0$ is a pre-exponential factor that could be derived from the molecular partition functions in both the bulk and the adsorbed phases. $b_0$ is often considered independent of the adsorption energy $\epsilon_{a,i}$ [16].

The adsorption energy distribution (AED) functions, $F(\epsilon)$, of the Bilangmuir, Trilangmuir and Quadrilangmuir are the sums of two, three *or* four Dirac functions, respectively:

$$F(\epsilon) = q_{s,1}\delta(\epsilon - \epsilon_{a,1}) + q_{s,2}\delta(\epsilon - \epsilon_{a,2}) \tag{7}$$

or

$$F(\epsilon) = q_{s,1}\delta(\epsilon - \epsilon_{a,1}) + q_{s,2}\delta(\epsilon - \epsilon_{a,2}) + q_{s,3}\delta(\epsilon - \epsilon_{a,3}) \tag{8}$$

or

$$F(\epsilon) = q_{s,1}\delta(\epsilon - \epsilon_{a,1}) + q_{s,2}\delta(\epsilon - \epsilon_{a,2}) + q_{s,3}\delta(\epsilon - \epsilon_{a,3}) + q_{s,4}\delta(\epsilon - \epsilon_{a,4}) \tag{9}$$

These energy distributions are bimodal, trimodal or quadrimodal and all their modes have a width 0.

### 2.3. Calculation of the adsorption energy distributions

In practice, there are no homogeneous domains. Actual surfaces are neither homogeneous nor paved with homogeneous tiles, as was assumed so far. All domains are somewhat heterogeneous because (1) impurities (e.g., boron, iron) in the bulk adsorbent segregate to its external surface; and (2) the valences of the atoms at the surface of the solid are incompletely satisfied and are somewhat strained and stressed. Adsorbent surfaces are characterized by an adsorption energy distribution (AED) that may have several more or less well resolved modes, each mode having a finite width. The experimental isotherm on such a heterogeneous surface is the

sum of the isotherms on each one of the types of sites covering the surface. There are different possible mathematical approaches to calculate the affinity energy distribution (AED) or distribution of the adsorption energy constants on the surface [16–19]. In this work, we derived it directly from the raw adsorption data by using the expectation-maximization method [19], a method previously described in detail [7]. It does not introduce any information that is not contained in the data. This method assumes that the adsorption isotherm on each homogeneous type of sites is a Langmuir or a Jovanovic isotherm. Accordingly, the method affords the energy distribution on heterogeneous adsorbents but only if the adsorbate–adsorbate interactions are negligible. Note that the results of AED calculations in liquid-solid adsorption are reported as the distribution of the adsorption equilibrium constant. They are given here as plots of the density of adsorption sites versus the natural logarithm of the equilibrium constant [17,19]. The energy corresponding to a certain equilibrium constant can be derived from Eq. (6), which requires knowledge of the pre-exponential factor. Resorting to the equilibrium constant distribution or affinity distribution rather than to the true AED avoids fundamental difficulties in the estimation of this factor. It is important to stress that the difference between the adsorption energies corresponding to two different equilibrium constants can be calculated directly. It is simply derived from their ratio without any knowledge of the pre-exponential factor.

### 2.4. Modeling of desorption-band profiles in HPLC

The overloaded band profiles of phenol and caffeine were calculated, using the equilibrium-dispersive model (ED) of chromatography [1,20,21]. The ED model assumes instantaneous equilibrium between mobile and stationary phases and a finite column efficiency originating from an apparent axial dispersion coefficient, $D_a$, that accounts for the dispersive phenomena (molecular and eddy diffusion) and for the non-equilibrium effects that take place in a chromatographic column. The axial dispersion coefficient is:

$$D_a = \frac{uL}{2N} \tag{10}$$

where $u$ is the mobile phase linear velocity, $L$ the column length, and $N$ the number of theoretical plates or apparent efficiency of the column, measured under linear conditions, i.e., with a small sample size.

In this model, the mass balance equation for a single component is written:

$$\frac{\partial C}{\partial t} + u\frac{\partial C}{\partial z} + F\frac{\partial q^*}{\partial t} - D_a\frac{\partial^2 C}{\partial z^2} = 0 \tag{11}$$

where $q^*$ and $C$ are the stationary and mobile phase concentrations of the adsorbate at equilibrium, respectively, $t$ is the time, $z$ the distance along the column, and $F = (1 - \epsilon_t)/\epsilon_t$ is the phase ratio, with $\epsilon_t$ the total column porosity. $q^*$ is related to $C$ through the isotherm equation, $q^* = f(C)$.

#### 2.4.1. Initial and boundary conditions for the ED model

At $t = 0$, the concentrations of the solute and the adsorbate in the column are uniformly equal to zero, and the stationary phase is in equilibrium with the pure mobile phase. The boundary conditions used are the classical Danckwerts-type boundary conditions [1,22] at the inlet and outlet of the column.

#### 2.4.2. Numerical solutions of the ED model

The ED model was solved using a computer program based on an implementation of the method of orthogonal collocation on finite elements (OCFE) [23–25]. The set of discretized ordinary differential equations was solved with the Adams–Moulton method, implemented in the VODE procedure [26]. The relative and absolute errors of the numerical calculations were $1 \times 10^{-6}$ and $1 \times 10^{-8}$, respectively.

## 3. Experimental

### 3.1. Chemicals

The mobile phase used in this work was a mixture of methanol and water (25:75, v/v), both HPLC grade, purchased from Fisher Scientific (Fair Lawn, NJ, USA). The solvents used to prepare the mobile phase were filtered before use on an SFCA filter membrane, 0.2 μm pore size (Suwannee, GA, USA). Thiourea was chosen to measure the column hold-up volume. Phenol and caffeine were the only two solutes used in this study. Thiourea, phenol and caffeine were all obtained from Aldrich (Milwaukee, WI, USA).

### 3.2. Columns

The three columns used in this study (XTerra MS $C_{18}$, Resolve-$C_{18}$ and Resolve silica) were given by the manufacturer (Waters Corporation, Milford, MA, USA). They all have the same size 150 mm × 3.9 mm. The main characteristics of the bare porous silica and of the packing material used are summarized in Table 1. The hold-up times of these

Table 1
Physico-chemical properties of the $C_{18}$-bonded packed XTerra, Resolve and Symmetry column (150 mm × 3.9 mm)

| Column | Resolve | Symmetry | XTerra |
|---|---|---|---|
| Particle size (mm) | 5 | 5 | 5 |
| Pore size[a] (Å) | 90 | 86 | 120 |
| Pore volume[a] (ml/g) | 0.50 | 0.90 | 0.64 |
| Surface area[a] ($m^2$/g) | 200 | 346 | 176 |
| Total carbon (%) | 10.2 | 19.6 | 15.2 |
| Surface coverage (μmol/$m^2$) | 2.45 | 3.18 | 2.50 |
| Endcapping | No | Yes | Yes |
| Total column porosity[b] | 0.6273 | 0.6044 | 0.6384 |

[a] Data for the packings before derivatization.
[b] Data from thiourea injections in a methanol/water mobile phase (25/75, v/v).

columns were derived from the retention time of two consecutive thiourea injections.

### 3.3. Apparatus

The isotherm data were acquired using a Hewlett-Packard (Palo Alto, CA, USA) HP 1090 liquid chromatograph. This instrument includes a multi-solvent delivery system (tank volumes, 1 l each), an auto-sampler with a 250 μl sample loop, a diode-array UV- detector, a column thermostat and a data station. Compressed nitrogen and helium bottles (National Welders, Charlotte, NC, USA) are connected to the instrument to allow the continuous operations of the pump, the auto-sampler, and the solvent sparging. The extra-column volumes are 0.068 and 0.90 ml as measured from the auto-sampler and from the pump system, respectively, to the column inlet. All the retention data were corrected for this contribution. The flow-rate accuracy was controlled by pumping the pure mobile phase at 23 °C and 1 ml/min during 50 min, from each pump head, successively, into a volumetric glass of 50 ml. The relative error was less than 0.4%, so that we can estimate the long-term accuracy of the flow-rate at 4 μl/min at flow rates around 1 ml/min. All measurements were carried out at a constant temperature of 23 °C, fixed by the laboratory air-conditioner. The daily variation of the ambient temperature never exceeded ±1 °C.

### 3.4. Measurements of the adsorption isotherms by FA

The solubility of phenol and caffeine are approximately 90 and 30 g/l in a methanol/water solution of composition 25:75 (v/v), respectively. Accordingly the maximum concentrations used in FA were 76 and 24 g/l to avoid any precipitation in the instrument. For each compound, two master solutions were prepared, at 10 and 100% of the maximum concentration. Two consecutive FA runs were then performed starting from the lowest to the highest concentrations. One pump (A) of the HPLC instrument was used to deliver a stream of the pure mobile phase (methanol/water, 25:75, v/v), the second pump (B for the 10% solution, C for the 100% solution) a stream of the sample solution. The concentration of phenol or caffeine in the FA stream is determined by the concentration of the mother sample solution and the flow rate fractions delivered by the two pumps. The breakthrough curves were recorded at a flow rate of 1 ml/min, with a sufficiently long time delay between each breakthrough curve to allow for the complete re-equilibration of the column with the pure mobile phase. The injection time of the sample was fixed at 6 min for all FA steps in order to reach a stable plateau at the column outlet. To avoid recording any UV-absorbance signal larger than 1500 mAU and the corresponding signal noise for the highest concentrations, and keeping a large enough signal for the lowest concentrations, the detector signal was detected at 285 nm (10% solution) and 291 nm (100% solution) for phenol and at 294 and 305 nm for caffeine. In each case, the detector response was calibrated accordingly by using the UV absorbance at the plateau observed on the breakthrough curves.

## 4. Results and discussion

### 4.1. Adsorption of phenol on Resolve-$C_{18}$ and XTerra-$C_{18}$ columns

Phenol was used first because it had been shown earlier that it has a bimodal adsorption energy distribution on the endcapped Kromasil-$C_{18}$ column and a Bilangmuir adsorption isotherm [5,7–9]. Furthermore, the proportions of the surface occupied by the first and second types of sites have a similar order of magnitude in the methanol/water mobile phase used in this study (methanol/water, 25/75, v/v). For instance, the low-energy saturation capacity, $q_{s,1} = 1.5$ mol/l, is nearly twice the high-energy saturation capacity, $q_{s,2}$. Thus, phenol appears to be an excellent model compound to study the origin of the heterogeneity of silica-based RPLC packing materials.

Figs. 1 and 2 show the adsorption data and the AEDs obtained for the adsorption of phenol on XTerra-$C_{18}$ (no surface silanols, apolar adsorbent) and on Resolve-$C_{18}$ (large number of surface silanols, polar adsorbent), respectively. According to the data, the isotherm model best accounting for the adsorption data on both columns is the bimodal Bilangmuir model. The validity of this isotherm model was checked by comparing calculated and experimental band profiles, Figs. 3 and 4. The calculated profiles were derived using the equilibrium-dispersive model of chromatography. The efficiency was adjusted so that the apex of the two bands match. Note that the efficiencies are relatively weak because, in the numerical calculations, we assumed the injection of a rectangular profile. Actually, the injection profile has a diffuse boundary both at its front and at its rear, due to molecular dispersion inside the connecting tubes between the mixer and the column inlet. This effect is easily taken into account through the apparent dispersion coefficient $D_a$ of the equilibrium-dispersive model. The agreement obtained between experimental and calculated profiles is very good (Figs. 3 and 4), validating the physical reality of the Bilangmuir model in our study.

Surprisingly, the numerical values of the isotherm parameters calculated from the AED results and from the regression analysis of the data (Table 2) for the two columns are too close to suggest that the adsorption mechanisms on the two columns are different. It is noteworthy that the low-energy adsorption constant, $b_1$, is slightly higher on the Resolve-$C_{18}$ column than on the XTerra-$C_{18}$. On the other hand, the high-energy adsorption constant, $b_2$, is slightly lower for Resolve-$C_{18}$ than for XTerra- $C_{18}$. It must be noticed also that the two saturation capacities are very close, almost identical, for the two columns ($q_{s,1} \simeq 2.0$ mol/l and $q_{s,2} \simeq 0.7$ mol/l). This result supports the conclusion that only the $C_{18}$-bonded layer, not the bare surface of the

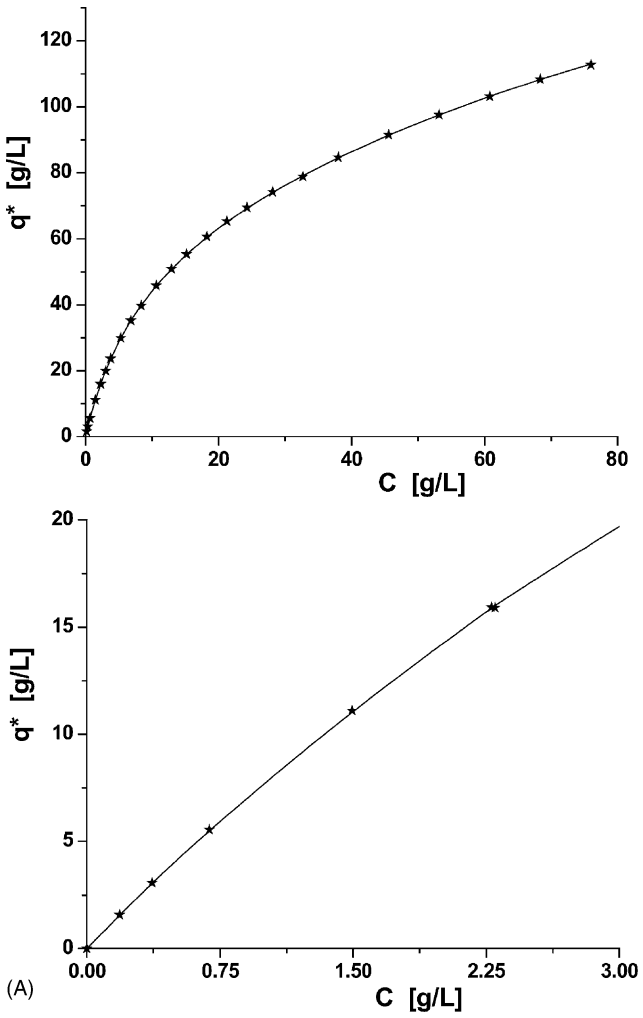


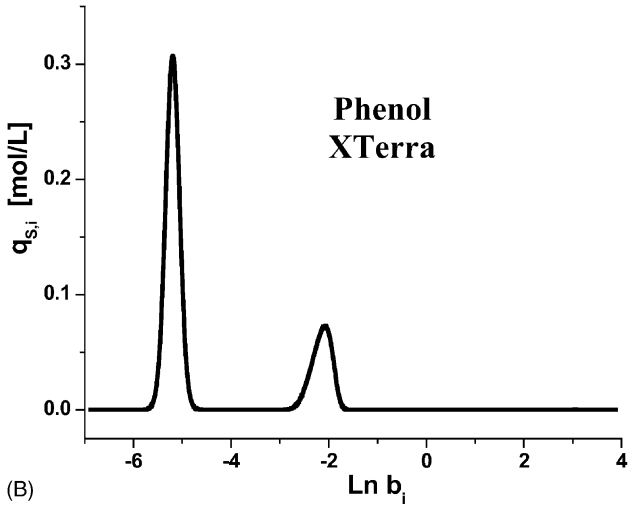


Fig. 1. (A) Adsorption isotherm data of phenol (star plot) and the best Bilangmuir model (solid line). XTerra-$C_{18}$ column, methanol/water (25/75, v/v), $T = 296$ K. (B) Affinity energy distribution of phenol calculated from the adsorption data using 100 millions iterations.

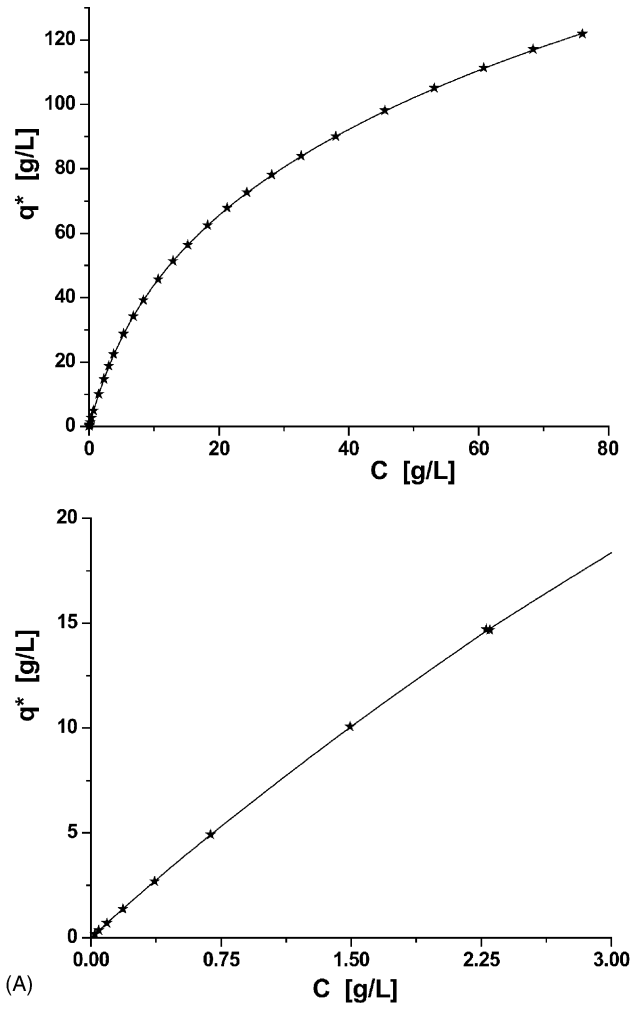


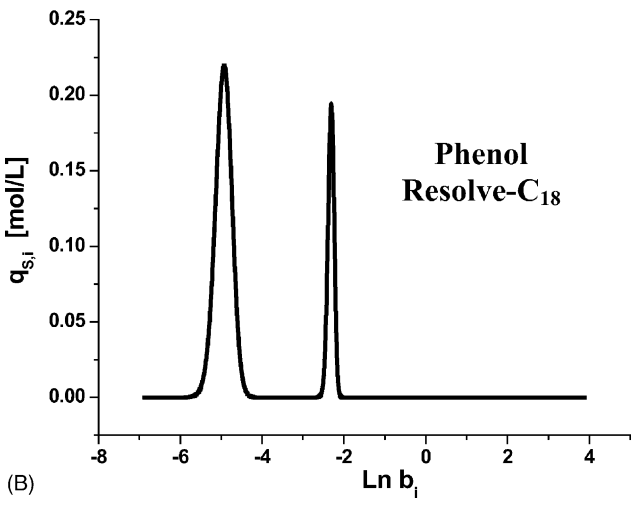


Fig. 2. (A) Adsorption isotherm data of phenol (star plot) and the best Bilangmuir model (solid line). Resolve-$C_{18}$ column, methanol/water (25/75, v/v), $T = 296$ K. (B) Affinity energy distribution of phenol calculated from the adsorption data using 100 millions iterations.

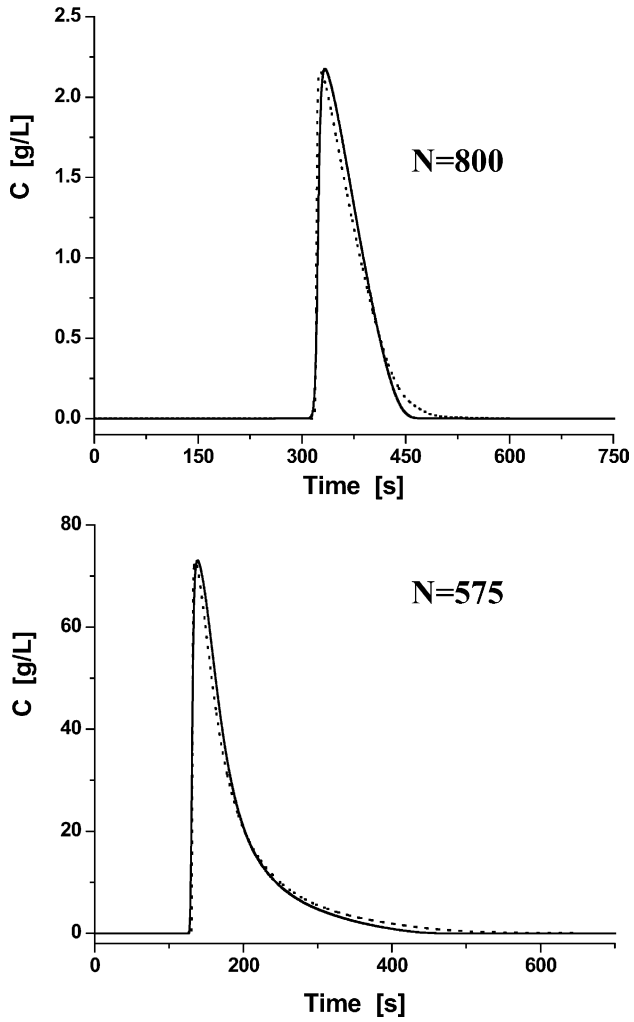


Fig. 3. Comparison between the experimental (dotted line) and simulated (solid line) band profiles of phenol on the Resolve-$C_{18}$ column. Methanol/water (25/75, v/v), $T = 296$ K. Calculation made by using the equilibrium-dispersive model of chromatography. Upper graph. Low column loading: injection of a 2.3 g/l solution during 60 s. Lower graph. High column loading: injection of a 76.0 g/l solution during 60 s.

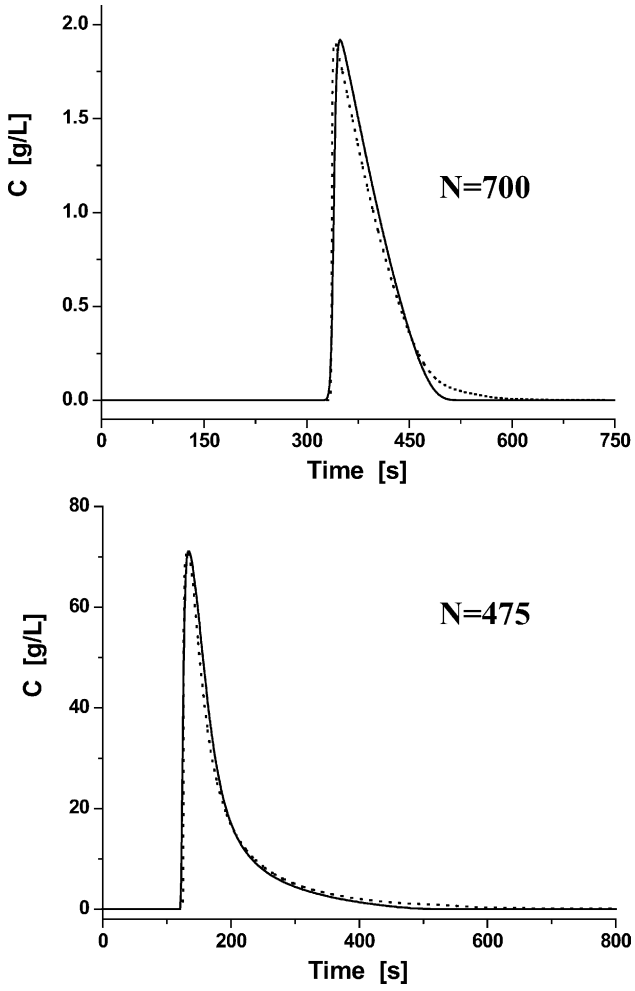


Fig. 4. Same as in Fig. 3 except on the XTerra-$C_{18}$ column.

adsorbent, is relevant in the adsorption mechanism of phenol in RPLC. Thus, the adsorption mechanism of phenol seems to be the same whether or not the surface of the stationary phase is endcapped or not. Note in Fig. 5 that the position of the peak of phenol is the same on both columns, suggesting that phenol does not adsorb on the bare Resolve silica. We

Table 2
Bilangmuir isotherm parameters obtained by the AED expectation-maximization calculations and by the regression analysis of the raw adsorption data

| | XTerra-$C_{18}$ | | | | Resolve-$C_{18}$ | | | | Symmetry-$C_{18}$[a] | | | |
|---|---|---|---|---|---|---|---|---|---|---|---|---|
| | Caffeine | | Phenol | | Caffeine | | Phenol | | Caffeine | | Phenol | |
| | AED | Fit | AED | Fit | AED | Fit | AED | Fit | AED | Fit | AED | Fit |
| $q_{s,1}$ (mmol/l) | 790 | 790 | 1990 | 1990 | 810 | 810 | 2010 | 2010 | 762 | 743 | 1413 | 1457 |
| $b_1$ (l/mol) | 2.75 | 2.89 | 0.52 | 0.54 | 3.72 | 3.36 | 0.67 | 0.65 | 2.43 | 2.64 | 0.73 | 0.98 |
| $q_{s,2}$ (mmol/l) | 90 | 80 | 680 | 650 | 110 | 140 | 670 | 690 | 42 | 33 | 654 | 563 |
| $b_2$ (l/mol) | 25.4 | 29.9 | 10.9 | 12.2 | 33.6 | 27.9 | 9.4 | 9.1 | 22.0 | 26.3 | 6.99 | 10.94 |
| $q_{s,3}$ (mmol/l) | – | – | – | – | 11 | 14 | – | – | – | – | – | – |
| $b_3$ (l/mol) | – | – | – | – | 267 | 237 | – | – | – | – | – | – |
| $q_{s,4}$ (mmol/l) | – | – | – | – | 0.28 | 0.30 | – | – | – | – | – | – |
| $b_4$ (l/mol) | – | – | – | – | 13550 | 13000 | – | – | – | – | – | – |

[a] Data previously acquired on a Symmetry column with a methanol/water mixture as for the mobile phase (30:70, v/v).

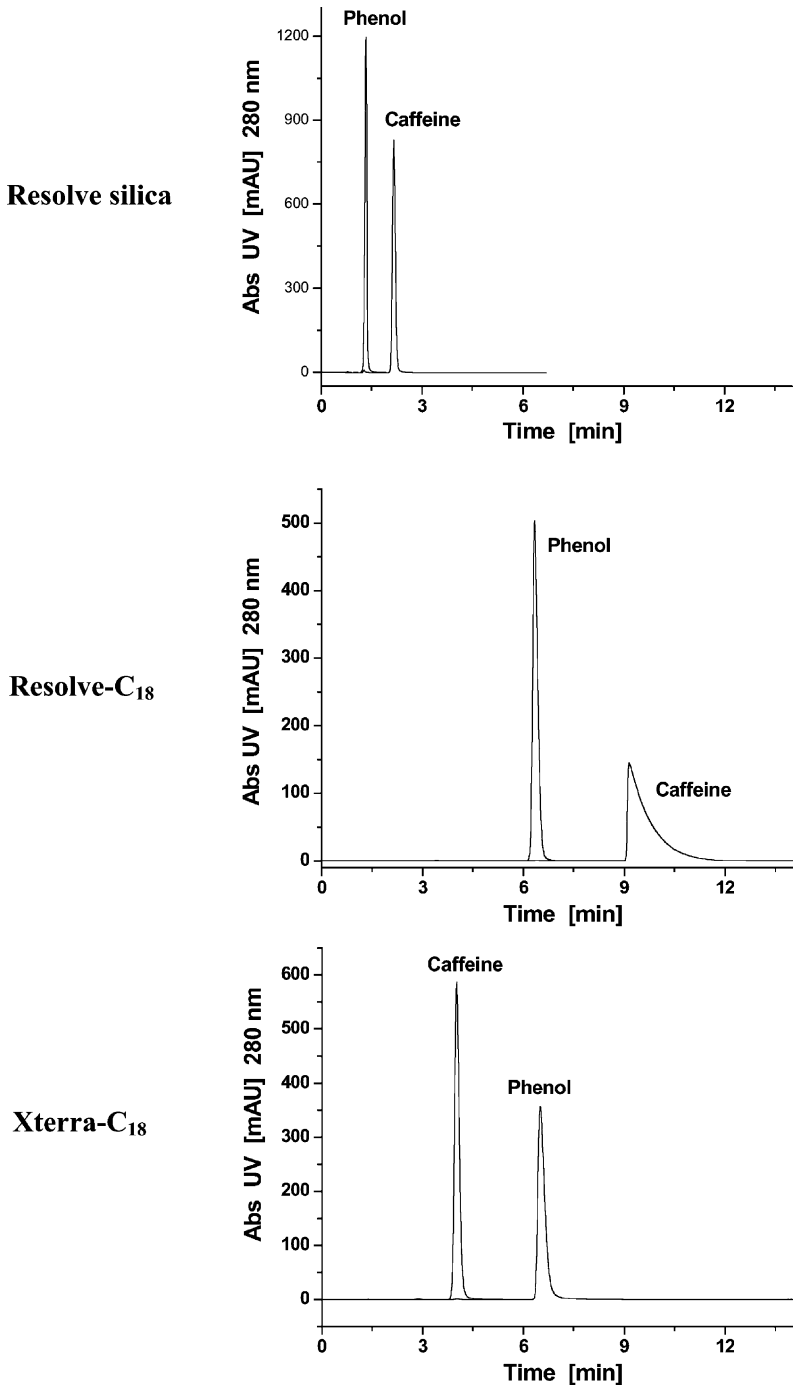


Fig. 5. Analytical injections of phenol and caffeine (20 μl, 1 g/l) on the underivatized Resolve silica, the derivatized Resolve-$C_{18}$, and the XTerra-$C_{18}$ columns (150 mm × 3.9 mm). Methanol/water (25/75, v/v), flow rate 1 ml/min, $T = 296$ K. *Note*: the reversal order of retention between the Resolve-$C_{18}$ and XTerra-$C_{18}$ columns and the strong peak tailing of caffeine by using the latter column.

checked out this result directly by injecting phenol (20 μl of a solution at 1 g/l) on a Resolve silica column under the same mobile phase conditions. The results are shown in Fig. 5. The retention factor of phenol on the underivatized Resolve column is less than 0.2. Assuming a monolayer saturation capacity of 2 mol/l (the same as for the Resolve-$C_{18}$ column), leads to an adsorption constant $b_{\text{resolve}}$ smaller than 0.16 l/mol. By contrast, the two adsorption constants measured on Resolve-$C_{18}$ are much larger ($b_1$ and $b_2$ are approximately 0.6 and 10 l/mol, respectively). This demonstrates that the retention of phenol on Resolve-$C_{18}$ cannot arise from any strong interactions between the bare silica surface of Resolve-$C_{18}$ and the phenol molecules. Even were we to assume a four-fold error on the saturation capacity of Resolve silica, this would explain the participation of the bare silica surface of Resolve-$C_{18}$ to only the weakest

interactions taking place on sites 1. This confirms the conclusions of an earlier work [10] where we reported that the adsorption of phenol on six different brands of RPLC columns was localized at the top surface of the $C_{18}$-bonded layer (adsorption mechanism on sites 1) and inside the layer (partition mechanism on sites 2)

### 4.2. Adsorption of caffeine on Resolve-$C_{18}$ and XTerra-$C_{18}$ columns

Caffeine is slightly less acidic than phenol. The pH of 5 mM solutions of caffeine and phenol in pure water, at 25 °C, are approximately 6.9 and 6.0, respectively. The molecule is larger, with a molecular weight of 194.2 Da versus 94.1 Da for phenol, and more hydrophobic. We might expect a stronger interaction between caffeine and the bare surface silanols of the Resolve-$C_{18}$ adsorbent and stronger interactions with the $C_{18}$ chains. Two silanol acidities were reported with p$K_a$ of 3.66 and 6.45, in almost equivalent proportions (50%) [11]. Yet, phenol and the less soluble caffeine have similar retention factors, a phenomenon which was explained previously [10].

#### 4.2.1. Adsorption of caffeine on the XTerra-$C_{18}$ column

Previous studies on the adsorption of caffeine were made on various brands of $C_{18}$-bonded silica phases, using a similar mixture of methanol and water as the mobile phase (30/70, v/v). The results showed that the same adsorption mechanism takes place for caffeine and phenol [10]. The Bilangmuir isotherm was the best model to account for the adsorption data of either compound. The main difference was the much lower saturation capacity of the high-energy sites for caffeine. This was explained by a size exclusion effect of the larger caffeine molecules from the network of $C_{18}$ chains bonded to the silica surface. While they account for between 28 and 43% of the total saturation capacity of the column for phenol, the high-energy sites account for only between 4 and 7% of the saturation capacity for caffeine [10]. Caffeine is less retained than phenol on the XTerra-$C_{18}$ column (Fig. 5). Fig. 6 shows the adsorption data of caffeine on the XTerra-$C_{18}$ column (Fig. 6A, symbols) and the AED (Fig. 6B) calculated from the adsorption data (in water/methanol 25:75, v/v). The AED obtained has two relatively narrow modes. Finally, Fig. 7 illustrates the good agreement between the experimental band profiles of caffeine and the profiles calculated from the Bilangmuir isotherm model (the parameters are in Table 2). All these results confirm the validity of the Bilangmuir model to account for the adsorption mechanism of caffeine on this new, low polar stationary phase.

The relative proportion of the high-energy sites accessible to caffeine is markedly higher on XTerra-$C_{18}$ than on conventional $C_{18}$-silica columns. The surface area of the high-energy sites visited by caffeine accounts for nearly 12% of its total column saturation capacity ($q_{s,1} \simeq 0.8$, $q_{s,2} \simeq 0.1$ mol/l) while it is 25% for phenol ($q_{s,1} \simeq 2.0$,

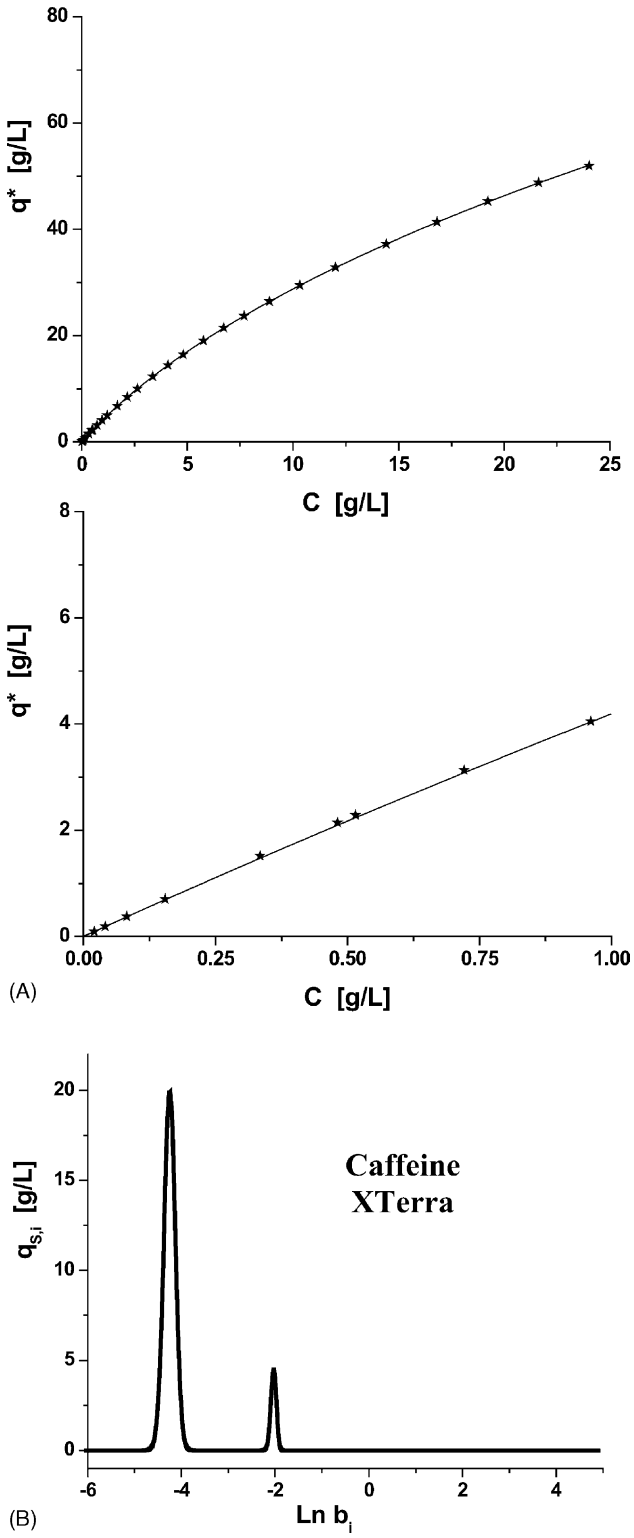


Fig. 6. (A) Adsorption isotherm data of caffeine (star plot) and the best Bilangmuir model (solid line). XTerra-$C_{18}$ column, methanol/water (25/75, v/v), $T = 296$ K. (B) Affinity energy distribution of caffeine calculated from the adsorption data using 100 millions iterations.

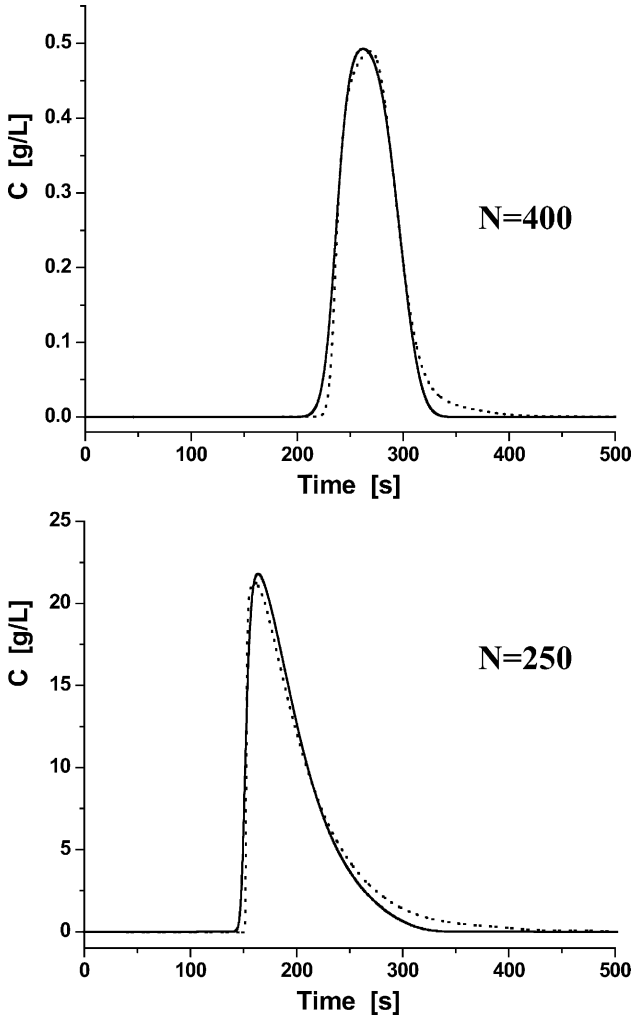


Fig. 7. Same as in Fig. 4 except with caffeine as the solute. Note that caffeine is eluted before phenol.

$q_{s,2} \simeq 0.7$ mol/l), as shown in Table 2. This difference might be explained by the significantly lower density of the $C_{18}$-chains on XTerra-$C_{18}$ (2.50 μmol/m$^2$) compared to that on the conventional brands of monomeric $C_{18}$ silica previously used [10], i.e., Hypersil (3.15 μmol/m$^2$), Waters Symmetry (3.20 μmol/m$^2$), Phenomenex (3.33 μmol/m$^2$), and Kromasil (3.59 μmol/m$^2$). Analyte molecules can more easily penetrate between the chains inside a less dense chain thicket. This is consistent with caffeine having a larger saturation capacity for the high-energy sites on XTerra-$C_{18}$ than on Symmetry-$C_{18}$ (0.09 versus 0.04 mmol/l) while its saturation capacities for the low-energy sites is the same on both columns (0.8 mmol/l). Also consistent with the relative hydrophobicity and size of the molecules of the two compounds studied are the values of their adsorption constants and saturation capacities. The values obtained for $b_1$ and $b_2$ for caffeine are approximately 5 and 2.5 times larger than the corresponding values measured for phenol, respectively. The values of $q_{s,1}$ and $q_{s,2}$ are about 2.5 and 8 times smaller for caffeine than for phenol. This confirms the similarity of the adsorption mechanisms of caffeine and phenol on the low-energy sites, because the ratio of their respective molecular weights (2.1) is close to 2.5. On the other hand, caffeine is partially excluded from the partitioning high-energy sites to which phenol has complete access. We might even conclude from the $b_1$ to $b_2$ ratios (5 and 2.5, respectively) that phenol is fully embedded while caffeine is only half-buried in the high-energy sites.

#### 4.2.2. Adsorption on Resolve-$C_{18}$ column

By contrast to its behavior on most other RPLC stationary phases, caffeine is more retained than phenol on Resolve-$C_{18}$ and its peak tails strongly. On the basis of the selectivity between caffeine and phenol ($\alpha_{C/P}$), Tanaka et al. [28] proposed to classify RP-HPLC columns. With an $\alpha_{C/P}$ of about 2 (See Fig. 5), Resolve-$C_{18}$ corresponds to a standard non-endcapped material prepared from a monofunctional silane, which is actually the case, but with a surface coverage ranging between 0.90 and 1.34 μmol/m$^2$. This material should exhibit a strong hydrogen bonding capacity. Actually, the measured chain density is about 2.5 μmol/m$^2$, which is far more than the value predicted by Tanaka. Conversely, with the actual chain density measured, we should observe a value of $\alpha_{C/P}$ close to unity, that is the coelution of phenol and caffeine. This result is not consistent with the assumption of a hydrogen bonding mechanism.

Fig. 8A shows its adsorption isotherm data. Comparison to Fig. 6A would suggest a saturation capacity higher for Resolve-$C_{18}$ than for XTerra-$C_{18}$. This is not supported by the values of the isotherm parameters (Table 2). The effect is explained by the higher values of the equilibrium constants (Table 2) which make higher the amount adsorbed on the column at equilibrium for a given concentration in the mobile phase, especially at low concentrations. For instance, at a concentration of 0.5 g/l in the mobile phase, the adsorbed amount on the Resolve-$C_{18}$ column is about twice that adsorbed on the XTerra-$C_{18}$ column. At 25 g/l, this ratio drops to 1.35. There is no similar effect for phenol, for which the equilibrium constants on the two columns are much closer. This difference in the equilibrium constants explains why phenol has about the same retention time on both columns while caffeine is eluted earlier than phenol on XTerra-$C_{18}$ and later on Resolve-$C_{18}$. These conclusions are confirmed by the good agreement between the experimental band profiles of caffeine and the calculated band profiles from the Bilangmuir isotherm model shown in Fig. 9

These observations suggest that additional interactions take place between caffeine and Resolve-$C_{18}$ at low concentrations that do not exist for phenol. Such interactions must be high-energy interactions. The existence of these interactions is confirmed by the AED reported in Fig. 8B. A quadrimodal energy distribution was found in this case. The two low-energy bands are physically consistent with those previously measured on XTerra-$C_{18}$ and with those observed for phenol on Resolve-$C_{18}$. The two corresponding types of sites have the same physical nature, whether

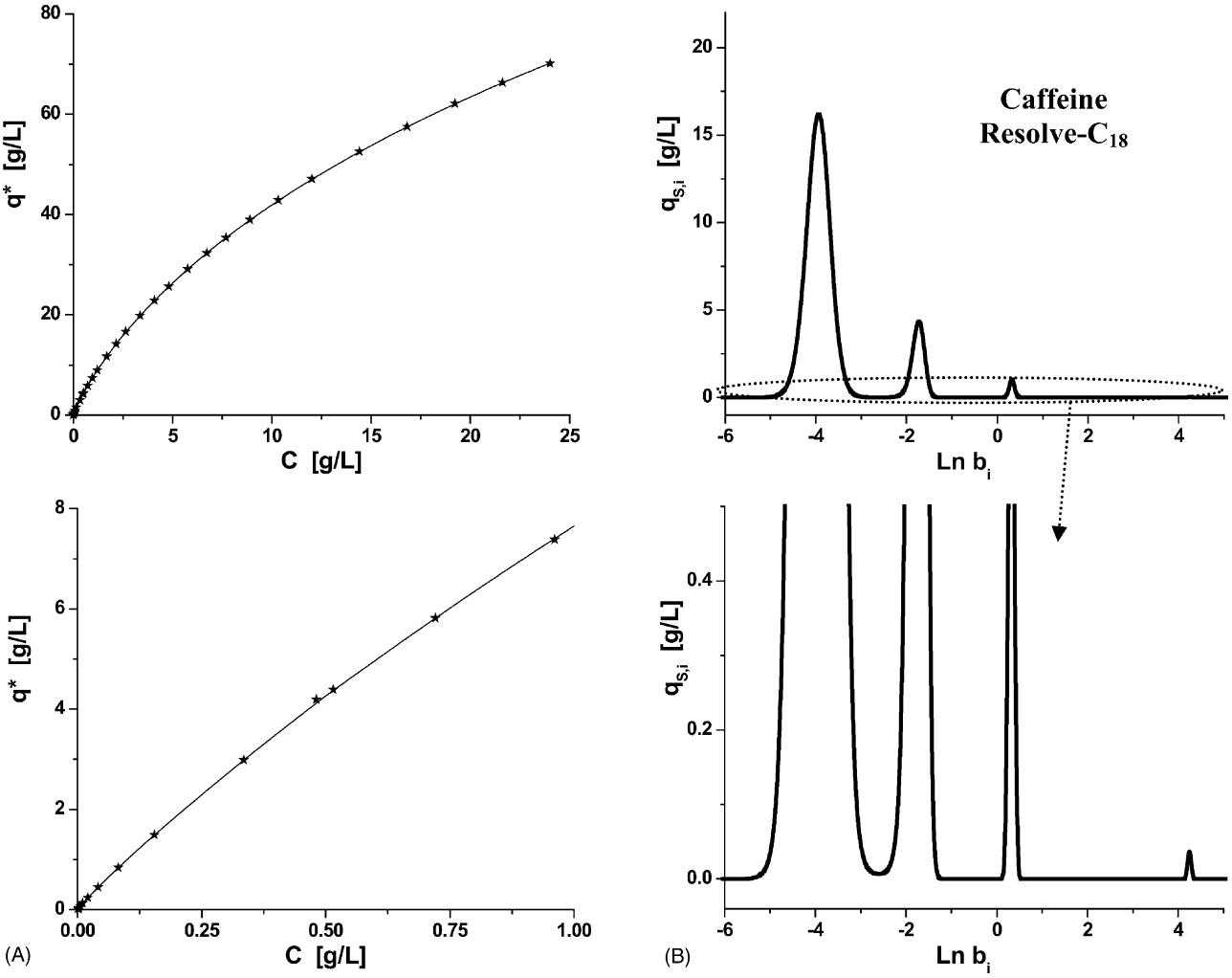


Fig. 8. (A) Adsorption isotherm data of caffeine (star plot) and the best Quadrilangmuir model (solid line). Resolve-$C_{18}$ column, methanol/water (25/75, v/v), $T = 296$ K. *Note*: the enhanced isotherm curvature and the higher amount adsorbed for caffeine concentrations below 1 g/l by comparison to Fig. 6A. (B) Affinity energy distribution of caffeine calculated from the adsorption data using 100 millions iterations. *Note*: the existence of two additional adsorption energies in the high-energy range.

the RPLC column is apolar (XTerra-$C_{18}$) or highly polar (Resolve-$C_{18}$). They must be located in and/or on the $C_{18}$ layer, thus they are the adsorption sites of types 1 and 2 described in the precedent section. This is consistent with the similarity of the estimates derived for each of the parameters $q_{s,1}$, $q_{s,2}$, $b_1$, and $b_2$ (Table 2) on the two columns.

As expected from the equilibrium isotherm data (the isotherm has a marked curvature at low concentrations, see Fig. 8a) and the chromatograms in Fig. 5, there are also two high energy bands predicted by both the AED calculation and the regression analysis. The corresponding saturation capacities $q_{s,3}$ and $q_{s,4}$ are much smaller that those of the two lower energy modes, 12 mmmol/l and 0.3 mmol/l, respectively. However, their effect on the isotherm behavior is significant because the adsorption constants $b_3$ and $b_4$ are high, 250 and 13,000 l/mol. This means that they are saturated at relatively low concentrations of caffeine in the mobile phase, which explains the significant curvature of the isotherm below 1 g/l (cf. Fig. 8A and 8A) and the tailing of the caffeine peak in Fig. 5, tailing which, in this case, is of thermodynamic, not kinetic origin (because, even for the sample size used—20 μg—the two high energy sites are saturated, see parameters Table 2).

The AED of caffeine on Resolve-$C_{18}$ (Fig. 8B) shows that the interaction energies on the sites of types 2, 3, and 4 are respectively 5, 10, and 20 kJ/mol higher than the interaction energy on type 1 sites. In order better to understand the physical origin of the sites of types 3 and 4, we injected a small amount of caffeine (20 μl at 1 g/l) on the Resolve silica column (See Fig. 5). The retention factor of caffeine is about 1 and the peak is symmetrical. Assuming that the column has a saturation capacity of 1 mol/l, this would lead to an adsorption constant of about 2 l/mol, values of the same order of those found for the sites of type 1 on Resolve-$C_{18}$. Accordingly, the interaction of caffeine with the bare surface of the Resolve column cannot be responsible for any of the high-energy interactions observed on $C_{18}$-Resolve (ca 35, 250, and 13,000 l/mol).

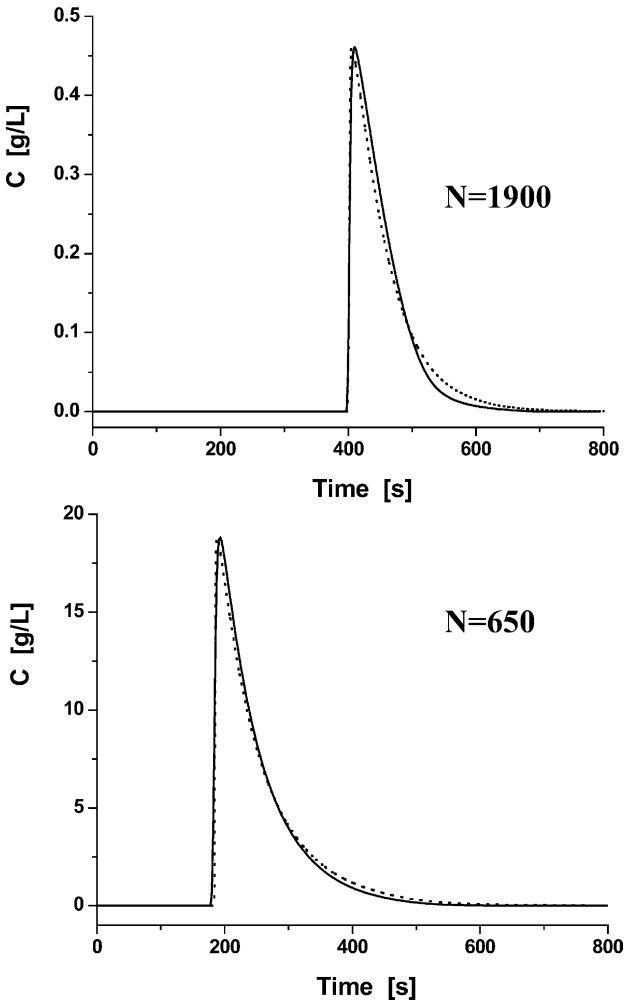


Fig. 9. Same as in Fig. 3 except with caffeine as the solute. *Note*: that caffeine is eluted after phenol.

An alternative explanation could be that caffeine does not interact with the silanols of the bare silica patches that are protected by molecules of water of the mobile phase and are located out of the $C_{18}$-bonded layer, but that it interacts with unprotected free silanols that are isolated within the hydrophobic $C_{18}$ environment, from which water molecules are excluded. Once the molecule of caffeine has penetrated the $C_{18}$ layer, it could form strong hydrogen bonding interactions with these isolated silanols. This interpretation is not acceptable, however, because such interactions are not observed with phenol, which is both a strong hydrogen bonding acceptor like caffeine and a strong hydrogen bonding donor. Indeed, it is well known that phenol is strongly retained on underivatized silica in NP-HPLC (e.g., with *n*-hexane as the mobile phase). It would also be inconsistent to assume that caffeine has an easier access than phenol to silanol groups isolated in the alkyl layer when its molecule is twice larger than phenol's.

The same conclusion as applied earlier for the adsorption of phenol (see earlier and [10]) can be drawn. The high-energy sites observed on stationary phases that have not been endcapped are probably related to the heterogeneity of the $C_{18}$-bonded layer structure in which the analyte may penetrate more or less deeper. They do not seem to be compatible with interactions with the free silanol groups.

It is more reasonable to state that caffeine may visit four different types of sites on Resolve-$C_{18}$:

(i) The most abundant type 1 sites, on which a simple adsorption mechanism takes place. The surface of contact between the chains and the adsorbate molecules is minimal. The adsorption constant is relatively low at 3.5 l/mol. The sites consist of $C_{18}$ chains probably collapsed on the silica surface or slightly swollen by a few molecules of methanol.

(ii) A second type of sites has a density that is one order of magnitude less than that of the sites of type 1. The molecules of caffeine are likely to be half-buried between $C_{18}$ chains. The adsorption energy on these sites is approximately 5 kJ/mol higher than on type 1 sites.

(iii) A third type of sites has a density that is two orders of magnitude lower than that of the type 1 sites. When adsorbed on these sites, the molecules of caffeine are completely embedded between $C_{18}$ chains. The adsorption energy on these sites is approximately 5 kJ/mol higher than on type 2 sites, hence 10 kJ/mol higher than on the sites of the first type.

(iv) The sites of the fourth type are far fewer than those of the three other types. Their density is approximately 40 times lower than that of the sites of type 3. This very small saturation capacity and the very high adsorption energy on these sites (10 kJ/mol higher than on type 3 sites) may render their existence questionable. However, we have never observed previously any peak such as the fourth peak in Fig. 8B in any AED calculated so far. It seems highly unlikely that this peak is an artifact. We have no adsorption mechanism to suggest in this case.

The fundamental results presented above show that the high-energy sites observed for caffeine cannot be explained by the existence of any "active sites" involving polar groups bound to the surface of Resolve-$C_{18}$. This conclusion is also supported by the results of adsorption experiments carried out with an endcapped $C_{18}$ bonded monolithic column [27]. Since Chromolith is an endcapped material, we cannot expect that there are on its surface silanol groups that would be much less hidden and protected than are found on Resolve-$C_{18}$ The adsorption equilibrium data of the same two compounds as used in the present study, phenol and caffeine, were measured. However, in order to adjust their retention and maximize the accuracy of the frontal analysis measurements, a higher water content was chosen for the mobile phase, 85% instead of 75% (v/v). The results of the regression analysis of these data were supported by the AED derived from the same data. These AEDs are reported

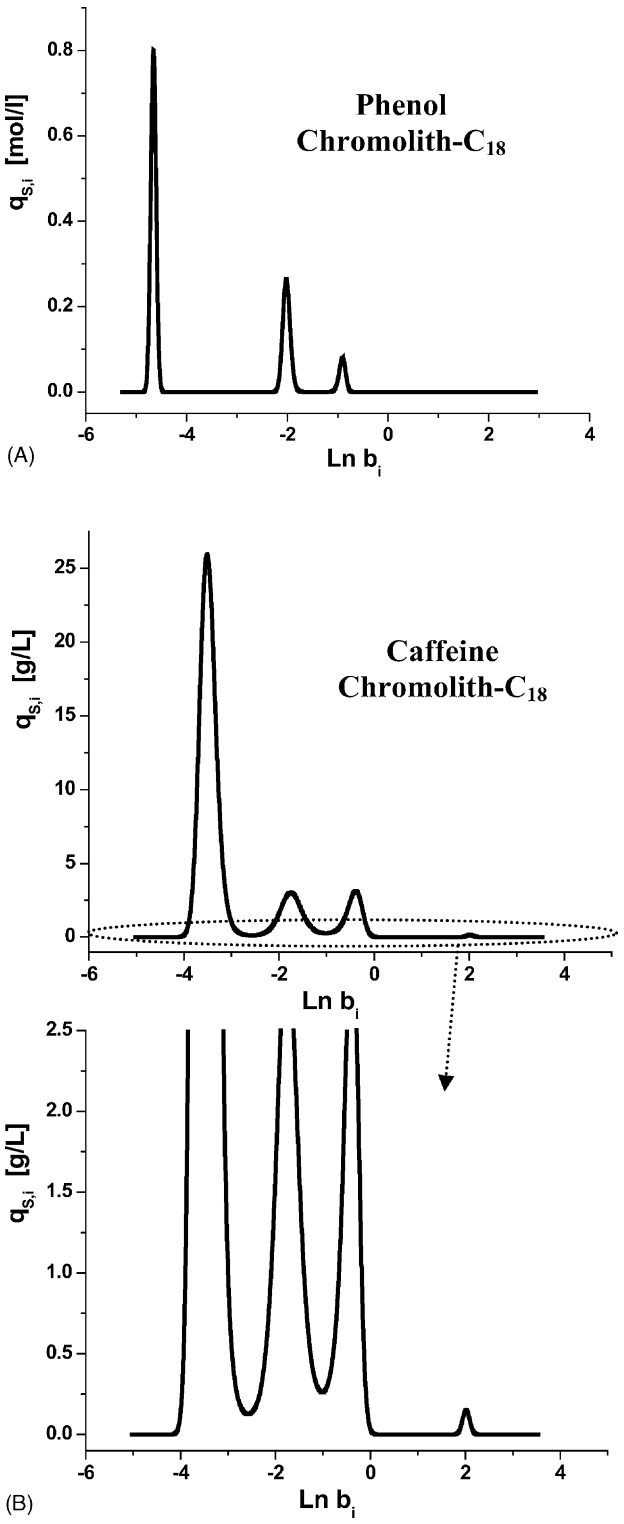


Fig. 10. (A) Adsorption energy distribution (AED) of phenol on an unused Chromolith-$C_{18}$ column. *Note*: the trimodal distribution. (B) AED of caffeine on the same monolithic column. *Note*: the quadrimodal distribution.

in Fig. 10A and B, for phenol and caffeine, respectively. Although the AED for phenol is now trimodal, both AEDs bear much similarity with those found in the present work. The peaks of caffeine and phenol on the monolithic column exhibited tailing, much as the caffeine peak in Fig. 5. These tailings which are observed at low concentrations ($\leq$1 g/l) are due to the heterogeneity of the adsorbent surface and to the corresponding equilibrium thermodynamics, not to any polar interaction and the corresponding slow mass transfer kinetics. Some structural heterogeneity of monolithic silica, e.g., macroscopic bonding non-uniformities, might explain the peak tailing observed.

## 5. Conclusion

Our results suggest that the presence of residual silanols on a silica surface does not significantly affect the chromatographic performance of the $C_{18}$-bonded adsorbent made from it provided that the sample molecules are small and neutral or mildly polar. Neither endcapping nor the preparation of a quasi-apolar bare silica surface are important prerequisite for the production of stationary phases giving satisfactory results for the separation of these analytes. The adsorption mechanism of phenol are exactly the same whether the adsorbent surface was the highly polar, silanol-group rich Resolve silica (Resolve-$C_{18}$ column) or the completely apolar XTerra material (XTerra-$C_{18}$ column). This is simply because phenol is barely adsorbed on neat silica from aqueous solutions of methanol. The retention of phenol is only due to its interactions with the heterogeneous $C_{18}$-bonded layer, on which there are two types of adsorption sites and which correspond to adsorption on the collapsed chains (low-energy sites) and partition with the network of these chains (high-energy sites), respectively.

In the case of larger molecules like caffeine, the absence of the classical endcapping of the $C_{18}$-bonded silica may enhance the heterogeneity of the surface energy distribution. The silanol groups may have no direct interactions with the analytes studied here, yet their presence could directly or indirectly influence the structure of the alkyl bonded layer and make it more heterogeneous. The AED of caffeine is bimodal on XTerra-$C_{18}$ but is quadrimodal on Resolve-$C_{18}$. The difference between the properties of these surfaces, in spite of the small contributions of the high-energy modes, is significant because it is not practical to use sample sizes so small that the Resolve-$C_{18}$ column behave linearly. The adsorption of caffeine on Resolve Silica is so weak that the tailing observed for analytical-size peaks of caffeine on Resolve-$C_{18}$, usually and abusively attributed to so-called “active” sites involving silanol groups and to a large contribution of a slow desorption kinetics from these sites to the mass transfer resistances, appears to be wrong. The physical origin of the high-energy sites is rather related to the existence of spots inside the $C_{18}$-bonded layer where molecules can bury themselves and become embedded. The values of the adsorption isotherm parameters that were determined in various adsorption studies on many RPLC stationary phases are consistent. The conclusions drawn here

extend to many RP-$C_{18}$ columns. This addresses the important and fundamental issue of the adsorption mechanism of molecules in RPLC using high water content or even pure water as the mobile phase. Accordingly, the hypothesis put forward in previous works [5,7,10,27], that the elution order of analytes must be understood on the basis of the analyte accessibility to buried sites rather than from the commonly applied and fragile concept of "polar active sites" or "slow desorption kinetics", is reinforced. Finally, the results obtained with phenol and caffeine suggest that, for these mildly polar compounds at least, the structure of the $C_{18}$ layer is far more important than the presence of some residual silanols. It is not clear at this stage what changes should be made to the nature of the silica surface used and to the procedure used to bind the $C_{18}$ chains. Yet, it is clear that their network should be more ordered. Possibly, the cross-linking of the chains, reducing the surface contribution of the sites of type 2 or higher, or the use of shorter chains (e.g., dodecyl or octyl rather than octadecyl chains) in which it would be more difficult for the analyte molecules to get buried, could result in better stationary phases. However, it cannot be denied at present that end-capping or the use *of* apolar substrate-surfaces can be most useful for the preparation of the high performance stationary phases needed for the analysis of basic or strongly basic compounds.

## Acknowledgements

This work was supported in part by grant CHE-02-44693 of the National Science Foundation, by Grant DE-FG05-88-ER-13869 of the US Department of Energy, and by the cooperative agreement between the University of Tennessee and the Oak Ridge National Laboratory. We thank Uwe Neue and Marianna Kele (Waters Corporation, Milford, MA, USA) for the generous gift of the columns used in this work and for fruitful and creative discussions.

## References

[1] G. Guiochon, S.G. Shirazi, A.M. Katti, Fundamentals of Preparative and Nonlinear Chromatography, Academic Press, Boston, MA, 1994.
[2] G. Guiochon, J. Chromatogr. A 965 (2002) 129.
[3] B. Lin, G. Guiochon, Modeling for Preparative Chromatography, Elsevier, Amsterdam, The Netherlands, 2003.
[4] A. Cavazzini, F. Gritti, K. Mihlbachler, G. Guiochon, Workshop Presented at the 16th International Symposium on Preparative/Process Chromatography, San Francisco, CA, 29 June–2 July 2003.
[5] F. Gritti, G. Götmar, B. Stanley, G. Guiochon, J. Chromatogr. A 988 (2003) 185.
[6] B.J. Stanley, S.E. Bialkowski, D.B. Marshall, Anal. Chem. 659 (1994) 27.
[7] F. Gritti, G. Guiochon, J. Chromatogr. A 995 (2003) 37.
[8] F. Gritti, G. Guiochon, J. Chromatogr. A 1010 (2003) 153.
[9] F. Gritti, J. Felinger, G. Guiochon, J. Chromatogr. A 1017 (2003) 45.
[10] F. Gritti, G. Guiochon, Anal. Chem. 75 (2003) 5726.
[11] A. Méndez, E. Bosch, M. Rosés, U.D. Neue, J. Chromatogr. A 986 (2003) 33.
[12] G. Guiochon, J. Chromatogr. A 965 (2002) 129.
[13] A. Felinger, G. Guiochon, J. Chromatogr. A 796 (1998) 59.
[14] G. Zhong, P. Sajonz, G. Guiochon, Ind. Eng. Chem. Res. 36 (1997) 506.
[15] D. Graham, J. Phys. Chem. 57 (1953) 665.
[16] M. Jaroniec, R. Madey, Physical Adsorption on Heterogeneous Solids, Elsevier, Amsterdam, 1988.
[17] R.J. Umpleby II, S.C. Baxter, Y. Chen, R.N. Shah, K.D. Shimizu, Anal. Chem. 73 (2001) 4584.
[18] J. Toth, Adsorption, Marcel Dekker, New York, NY, 2002.
[19] B.J. Stanley, G. Guiochon, J. Phys. Chem. 97 (1993) 8098.
[20] D.M. Ruthven, Principles of Adsorption and Adsorption Processes, Wiley, New York, NY, 1984.
[21] M. Suzuki, Adsorption Engineering, Elsevier, Amsterdam, The Netherlands, 1990.
[22] P.W. Danckwerts, Chem. Eng. Sci. 2 (1953) 1.
[23] K. Kaczmarski, M. Mazzotti, G. Storti, M. Morbidelli, Comput. Chem. Eng. 21 (1997) 641.
[24] K. Kaczmarski, Comput. Chem. Eng. 20 (1996) 49.
[25] K. Kaczmarski, D. Antos, J. Chromatogr. A 862 (1999) 1.
[26] P.N. Brown, A.C. Hindmarsh, G.D. Byrne, Procedure available from http://www.netlib.org.
[27] F. Gritti, G. Guiochon, J. Chromatogr. A 1028 (2004) 105.
[28] K. Kimata, K. Iwaguchi, S. Onishi, K. Jinno, R. Eksteen, K. Hosoya, M. Araki, N. Tanaka, J. Chromatogr. Sci. 36 (1997) 506.